Sonic hedgehog is required for neural crest-dependent patterning of the intrinsic tongue musculature

Shigeru Okuhara, Anahid A. Birjandi, Hadeel Adel Al-Lami, Tomoko Sagai, Takanori Amano, Toshihiko Shiroishi, Karen J. Liu, Martyn T. Cobourne, Sachiko Iseki

Abstract

The tongue is a highly specialized muscular organ important for breathing, speech, taste and swallowing. The secreted signaling molecule Sonic hedgehog (Shh) is expressed in dorsal tongue epithelium from the initial developmental stage. In this study, we utilized a series of genetic approaches to investigate the role of Shh during mouse tongue formation. Temporal-specific global deletion of *Shh* demonstrated a functional requirement for normal patterning of the intrinsic tongue muscles and establishment of the lingual tendon. These defects were reproduced in the mutant with a specific loss of signaling in oropharyngeal epithelium by a *Shh cis*-enhancer. In these mutants, *Ptch1* was lost in the underlying cranial neural crest (CNC)-derived mesenchymal lineage. The importance of Shh was confirmed by generating tissue-specific deletions in the ciliopathy gene *Ofd1*, which transduces Shh signaling. These results revealed Shh roles in patterning of the mesodermal intrinsic tongue muscles through CNC-derived mesenchyme, including the lingual tendon.

Introduction

The tongue is a highly specialized muscular organ, which is required for normal mandibular growth and palatogenesis in the developing embryo and essential for airway maintenance, phonetic articulation, oral sensation and swallowing in post-natal life. Correct functioning of the tongue requires the cooperation of extrinsic and intrinsic muscles, tendons, neurons and a generous vasculature. Despite the functional importance of the tongue, comparatively little is known about the signaling events required to coordinate all these component structures to the development.

In the embryo, tongue primordia appear as paired swellings on the ventral wall of the pharyngeal arches at around embryonic day (E)10 in mice. These swellings grow and ultimately fuse with a medial lingual swelling to become a single midline structure in the floor of the early oral cavity. Myoblasts populate these early primordia following migration from the hypoglossal cord, a condensed region of mesoderm lying at the ventral edges of the occipital myotomes (Noden and West, 2006). The process of subsequent tongue development requires tissue interactions between the oropharyngeal

41 epithelium, cranial neural crest (CNC)-derived mesenchyme and myogenic mesoderm
42 (Parada et al., 2012).
43
44 Sonic hedgehog (Shh) is a secreted protein that plays a key role in diverse biological
45 events extending from early development through to post-natal tissue homeostasis
46 (Xavier et al., 2016; Peng and Joyner, 2015; Zuniga, 2015; Thesleff and Sharpe, 1997).
47 Signal transduction is coordinated primarily through direct ligand-dependent inhibition
48 of Patched-1 (Ptch1), a multi-span transmembrane protein that in the resting state
49 indirectly inhibits a further multi-span protein Smoothened (Smo), which is absolutely
50 required for transduction. These events are coordinated at the primary cilium and
51 ultimately lead to pathway activation through post-transcriptional modification of Gli
52 protein activity (Chang et al., 2016; Tabler et al., 2016). During embryonic development,
53 *Shh* is expressed in very specific domains such as the node, notochord and floor plate,
54 as well as in the limbs. Early expression of *Shh* in the midline is crucial for normal
55 craniofacial development with complete loss of *Shh* function leading to
56 holoprosencephaly (Gregory et al., 2015; Chiang et al., 1996) and a catastrophic failure

of orofacial patterning. More recent studies have begun to distinguish the individual spatio-temporal signaling functions of *Shh* during craniofacial development (Xavier et al., 2016). Removal of Hedgehog (Hh)-responsiveness from CNC-derived mesenchyme through deletion of *Smo* in CNC cells (*Wnt1-Cre*; $Smo^{flox/-}$) has demonstrated a requirement for Hh signaling in this population within the early facial processes from their commitment stage (Jeong et al., 2004). Significantly, the early facial processes are hypoplastic from E10.5 in these mice, and subsequently most CNC-derived cranial skeletal elements are impaired or aplastic, including a severely affected mandible associated with aglossia. In addition, deletion of *Shh* from E9.5 in an *Nkx2.5*-expressing cell lineage (*Nkx2.5Cre*; $Shh^{flx/ko}$), which overlaps that of *Shh* in oropharyngeal endoderm (Moses et al., 2001) also results in micrognathia and aglossia (Billmyre and Klingensmith, 2015). Whilst these studies demonstrate a clear role for *Shh* in establishment of the tongue primordia, they do not address potential later roles for *Shh* in patterning of the tongue tissues.

In this study, we have utilized a series of genetic approaches to investigate the relevance

of Shh signaling during tongue formation, focusing on the source, timing and effect on receiving tissues. We find that production of Shh ligand in the lingual epithelium up to E12.5 is crucial for normal patterning of the intrinsic musculature and that this occurs through signaling to CNC cells to differentiate lingual tendons. Our studies provide the understanding of tongue phenotypes seen in some patients with ciliopathies, such as *orofacial-digital-syndrome-1*, which include tongue clefting, cystic and hamartomatous changes, as well as cleft palate.

Results

Shh signaling is required for intrinsic muscle organization and tendon formation in the developing tongue

Shh is an early marker for tongue development, being expressed in dorsal epithelium of the lateral lingual swellings from E10.5 and upregulated in lateral regions of the primitive tongue by E11.0 before localizing to early placodal epithelium from E12 (Jung et al., 1999). We have investigated the contribution of *Shh* during tongue development with temporal abrogation of function in mutant mice. Specifically, we crossed $CreER^{TM}$ mice (Hayashi and McMahon, 2002) with a line harboring a conditional (floxed) Shh^{c} allele with *loxP* sites flanking exon 2 of the endogenous *Shh* locus (Dassule et al., 2000). After recombination, approximately half of the N-terminal signaling domain is removed from the Shh protein, rendering it non-functional. Following the maternal administration of tamoxifen between E10.5-12.5 and analysis three days later, there was evidence of disruption in anatomy of the tongue in mutant mice when compared to wild type (WT) (Figure 1A-D). In particular, significant disorganization of the intrinsic musculature within the tongue dorsum was present,

97 which was grossly dependent upon the timing of signal loss (Figure 1E-H). In mice
98 treated with tamoxifen at E10.5, the normal striated architecture of the intrinsic muscles
99 was completely lost, whilst deletion at later stages resulted in a progressively less severe
100 myogenic patterning phenotype (Figure 1E-H). However, *in situ* hybridization for the
101 myoblast marker *Myod1*, in WT and mutant embryos suggested that myoblast
102 differentiation had occurred in both the intrinsic and extrinsic musculature, even in the
103 most severely affected mutants, but that organization of the myotubes was defective
104 (Figure 1I-L).
105
106 CNC-derived mesenchyme within the tongue has been suggested to act as a scaffold
107 during the organization of myoblasts and myotubes (Parada et al., 2015). The tongue
108 musculature is patterned through the formation of tendons, which include the
109 aponeurosis and lingual septum, which forms within the tongue dorsum as a flat broad
110 vertical sheath of midline fibrous tissue. We investigated expression of the *Scleraxis*
111 (*Scx*) transcription factor, which is an early marker of tenocyte differentiation
112 (Schweitzer et al., 2001) in WT and mutant embryos at E14.5 (Figure 1M-P). As

113 expected, *Scx* was strongly expressed in the developing midline lingual septum in WT
114 (Han et al., 2012) with more widespread low-level expression in lateral regions of the
115 tongue dorsum. In addition, there was strong bilateral midline expression at sites of
116 tendon formation associated with the paired genioglossus and geniohyoid muscle bellies
117 superiorly and inferiorly, respectively (Figure 1M). In contrast, whilst *Scx* expression
118 was present in the developing genioglossus and geniohyoid tendons of the mutant, there
119 was a loss of expression in the midline septum and significant downregulation in lateral
120 regions of the dorsum in embryos injected at E10.5 (Figure 1N). However, this
121 expression was progressively increased in embryos exposed to later injection at E11.5
122 and 12.5, respectively (Figure 1O and P). Collectively, these data demonstrate an
123 important role for Shh in mediating normal organization of the intrinsic musculature of
124 the tongue, including tendon architecture.
125

126 **Shh in the oropharyngeal epithelium is required for intrinsic muscle**
127 **organization and tendon formation**

128 The expression of *Shh* in epithelium extending from the oral cavity to the gut is

129 regulated during development by the conserved long-range *cis*-regulatory enhancers,
130 *MRCS1, MFCS4* and *MACS1* located 600 to 900 kb upstream of the mouse *Shh* locus
131 (Sagai et al., 2009). *MFCS4* is responsible for regulating the majority of *Shh* expression
132 in oropharyngeal epithelium from which the incisor tooth bud, pituitary fossa, soft
133 palate, tympanic tube, tongue, epiglottis and arytenoid cartilages have initiated
134 development by E11.0. Targeted deletion of *MFCS4* in mice results in shortening of the
135 soft palate as well as deformation of the epiglottis, arytenoid and tongue, although the
136 size of tongue and mandible are normal (Sagai et al., 2009).
137
138 In order to further define the influence of Shh signaling in tongue development we
139 analyzed compound heterozygous $Shh^{+/-}$; $MFCS4^{-/+}$ mice, where Shh signaling in the
140 developing tongue is clearly decreased by E11.75, as demonstrated by expression of
141 *Shh* and *Ptch1* (Figure 2A-D). At this stage of development, *Myf5*-positive myoblasts
142 have reached the developing tongue dorsum from the occipital somites in WT and
143 $Shh^{+/-}$; $MFCS4^{-/+}$ embryos (Figure 2F and G), confirming that myoblast migration into
144 the tongue primordium is not affected by loss of Shh signaling. The presence of

145 myoblast differentiation was also confirmed in the WT tongue through detection of
146 *Myod1* in anterior and posterior regions at E11.5 (Figure 2Ha and Hp) with myoblasts
147 present anteriorly expressing *Myod1*, but not desmin at this stage (Figure 2Ha and Ja);
148 whilst those more posteriorly expressed both markers (Figure 2Hp and Jp). Since
149 desmin is a key subunit of the intermediate filaments required for contraction, these
150 observations suggest that lingual myoblast differentiation progresses from posterior to
151 anterior during normal tongue development. This expression pattern was not altered in
152 $Shh^{+/-}$; $MFCS4^{-/+}$ mutants (Figure 2Ia, Ip, Ka, and Kp). These observations were
153 maintained at E12.5 and confirmed by quantitative RT-PCR (Figure 2E). At E13.5,
154 myotube organization was disrupted and distinct in the superior longitudinal, vertical
155 and transverse intrinsic muscles (Figure 2L and M) compared to lateral regions, where
156 the extrinsic styloglossus muscle runs. In contrast, vascularization and innervation did
157 not appear to be affected in the mutant (Figure 1 - figure supplement 1). As we found in
158 $CreER^{TM}$; $Shh^{fl/fl}$ embryos, $Shh^{+/-}$; $MFCS4^{-/+}$ mice failed to develop *Scx*-positive tendons
159 for the intrinsic muscles at E13.5 (Figure 2N and O) despite clear expression in the
160 developing genioglossus muscle within the symphyseal region of the mandible (Figure

161 2N and O arrowheads). *Scx* expression in lateral regions was identified in some *Shh*$^{+/-}$;

162 *MFCS4*$^{-/+}$ embryos (Figure 2O arrows).

163

164 **Shh signaling in the developing tongue targets CNC cells via the primary**

165 **cilium**

166 Given that myoblast migration and differentiation was not seemingly affected in the

167 absence of Shh signaling in lingual epithelium, but tendon formation specifically was;

168 we hypothesized that the direct target of Shh was CNC cells. We therefore investigated

169 the spatial relationship between *Ptch1*-positive cells, CNC cells and myoblasts in the

170 developing tongue (Figure 3A-E). The detection of beta-galactosidase, *Ptch1* and *Myf5*

171 transcripts in adjacent sections of the developing tongue at E12.5 in *Wnt1-Cre; R26R*

172 embryos indicated that CNC-derived mesenchymal cells expressed *Ptch1* and was

173 therefore a primary target tissue of Shh signal transduction during tongue development.

174

175 Shh ligand binds to the primary receptor Ptch1, which is located on the primary cilium

176 of receiving cells. Cilia are recognized as key cellular organelles necessary for normal

177 Hh signal transduction in vertebrates, and mutations in the basal body gene *Ofd1*
178 localized on X chromosome lead to a ciliogenesis defect and loss of Shh signal
179 reception (Al-Lami et al., 2016; Ferrante et al., 2006). In human subjects affected by
180 loss-of-function *OFD1* mutations there are multiple craniofacial anomalies, including
181 cleft palate and significant tongue defects, which include clefting, cystic formation and
182 hamartoma. The generation of *Wnt1-Cre; Ofd*$^{fl/Y}$ mice with deletion of *Ofd1* in
183 CNC-derived mesenchymal cells led to a reduction of Shh signaling in the tongue, as
184 demonstrated by decreased levels of *Ptch1* expression at E11.5 and 12.5 (Figure 3F and
185 G; I and J, respectively). In contrast, deletion of *Ofd1* in the mesoderm-derived cells
186 (*Mesp1-Cre; Ofd*$^{fl/Y}$) did not affect *Ptch1* expression in the tongue (Figure 3H and K).
187 Significantly, in *Wnt1-Cre;Ofd*$^{fl/}$*Y* mice there was a complete loss of normal myotube
188 arrangement (Figure 3L and M) as well as severe hypoplastic tongue formation and only
189 clumps of *Myod1*-positive myotubes; whilst in *Mesp1-Cre;Ofd*$^{fl/}$*Y* mutants, myotube
190 arrangement was largely unaffected (Figure 3N). These observations suggest that
191 lingual tendon formation for intrinsic muscles of the tongue requires Shh signaling from
192 the ventral region of the pharyngeal arches.

193

194 **Lingual CNC-derived mesenchymal cell differentiation but not**

195 **proliferation is affected in *Shh*$^{+/-}$; *MFCS4*$^{-/+}$ mice**

196 We further analyzed CNC cell differentiation in *Shh*$^{+/-}$; *MFCS4*$^{-/+}$ mice. *Sox9* is a

197 marker for CNC cells as well as a common representative transcription factor for

198 chondrocyte, ligament cell and tenocyte differentiation (Spokony et al., 2002;

199 Mori-Akiyama et al., 2003). Upon Bmp-ligand stimulation, mesenchymal cells

200 differentiate into either cartilaginous or tendinous fates by maintaining or decreasing

201 *Sox9* transcription, respectively (Sugimoto et al., 20013. In WT tongues, there was an

202 increase in *Sox9* transcription between E11.75-12.75, with strong expression in the

203 future lingual septum-forming region, that has decreased by E13.75 (Figure 4A, C, and

204 E). In the mutant, *Sox9* was only weakly expressed at E12.75 (Figure 4B, D, and F).

205 Low levels of *Scx* expression was detected from E11.75 in the WT tongue in posterior

206 regions, but not anteriorly (Figure 4G and data not shown). At E12.75, an upregulated

207 M-shaped pattern of expression was seen (Figure 4I), which coincided with the

208 expression pattern in whole mount (Figure 4K). In contrast, there was little evidence of

209 *Scx* transcripts at E11.75 in *Shh*$^{+/-}$; *MFCS4*$^{-/+}$ embryos (Figure 4H) and only faint
210 expression at E12.75 (Figure 4J). Whole mount *in situ* hybridization of *Scx* in E12.75
211 *Shh*$^{+/-}$; *MFCS4*$^{-/+}$ embryos was consistent with these observations (Figure 4L).
212 Collectively, these observations suggested that during tenocyte differentiation from
213 CNC-derived lingual mesenchymal cells there is a transition stage at which, they
214 express both *Sox9* and *Scx*.
215
216 In accordance with the *Scx* expression pattern, *fibronectin* (*Fn1*) and *type I collagen*
217 (*Col1a1*), and *fibroblast growth factor receptor 1* (*Fgfr1*) were transcribed clearly in the
218 WT aponeurosis and septum (Figure 4M, O, and Q, respectively) whereas expression in
219 the *Shh*$^{+/-}$; *MFCS4*$^{-/+}$ tongue was weak and not well patterned (Figure 4N, P, and R).
220 *Desmin* expression was observed in both WT and *Shh*$^{+/-}$; *MFCS4*$^{-/+}$ tongue at E13.75
221 although it was disorganized in the latter (Figure 4S and T), which suggested relatively
222 normal myotube formation. Being suggested from the previous reports (Brent et al.,
223 2003, Brent et al., 2005, Sukegawa et al., 2000, Du et al., 2016), we hypothesized Fgf
224 signaling also contribute to tenocyte differentiation. To address this issue, we applied

225 recombinant human FGF18 in the developing tongue at E11.0 and run organ culture.
226 FGF18 induced stronger expression of *Scx* in genioglossus, as well as the strong broad
227 expression in the tongue mesenchyme (Figure 4U and V). *Sox9* transcription was not
228 altered by FGF18 application (Figure 4W and X).
229
230 We also studied cell proliferation activity in the early tongue mesenchyme at E11.75
231 and 12.75 in WT and *Shh*$^{+/-}$*; MFCS4*$^{-/+}$ embryos during which, tenocyte specification
232 occurs in CNC cells (Figure 4Y). Proliferative activity of CNC-derived mesenchyme
233 did not change between E11.75 and E12.75, whereas that of myoblasts was significantly
234 decreased in both WT and *Shh*$^{+/-}$*; MFCS4*$^{-/+}$ embryos, suggestive of active myotube
235 formation during this period. In contrast, no differences in cell death were found in WT
236 and *Shh*$^{+/-}$*; MFCS4*$^{-/+}$ embryos between E11.75 and 13.75 (data not shown).
237
238 **A functional tongue is required for secondary palate formation**
239 Previous studies have shown that approximately 14% of *MFCS4*$^{-/-}$ mice exhibit cleft
240 palate (Sagai et al., 2009), whilst compound heterozygous *Shh*$^{+/-}$*; MFCS*$^{+/-}$ mice have

241 full penetrance cleft palate and a short soft palate (Figure 5 - figure supplement 2).

242 Histological observation during palatogenesis revealed that palatal shelf elevation was

243 disturbed in the compound *Shh*$^{+/-}$*; MFCS*$^{+/-}$ heterozygote (Figure 5A-F). It has been

244 suggested that palatal shelf elevation and orientation requires coordination between

245 intrinsic factors within the shelves themselves and extrinsic factors such as the descent

246 of the tongue due to embryonic muscle movement, which would provide space in the

247 oral cavity for palate rotation (Iseki et al., 2007). In *Shh*$^{+/-}$*; MFCS4*$^{+/-}$ mice, the palatal

248 shelves were able to elevate and fuse in the midline (n=3) when explanted for organ

249 culture at E13.5, confirming that the cleft palate phenotype resulted from hindrance by

250 the tongue (Figure 5G and H).

251

252 Micro computed tomography (μCT) analysis on neonatal skeletons of compound

253 heterozygous *Shh*$^{+/-}$*; MFCS4*$^{-/+}$ mice showed a variety of skeletal defects in the

254 maxillary region (Figure 5 - figure supplement 3). In severe cases, an unfused sphenoid,

255 missing premaxilla and vomer and hypoplastic sphenoid tympanic bones were found.

256 However, no defects were identified in the mandible.

257

Discussion

A number of signaling pathways have been implicated in tongue formation but the timing and tissue interactions controlling muscle formation have not been well established (reviewed in Parada et al., 2012). *Shh* is expressed in the oropharyngeal epithelium and disruption of signaling in the pharyngeal endoderm prior to tongue morphogenesis (Billmyre and Klingensmith, 2015) or a loss of Hh responsiveness in CNC cells prior to migration (*Wnt1-Cre; Smo*$^{flox/KO}$) (Jeong et al., 2004) both result in aglossia. However, the phenotypic severity associated with both these mouse models precludes analysis of later patterning events in tongue development.

In this study, we show that Shh signaling directly induces formation of the lingual septum derived from CNC cells and that regulation through the *MFCS4* enhancer activated by E11.0 is essential for this process to occur. Removal of Shh signaling throughout the embryo from E10.5 by CreER-mediated site-specific recombination resulted in impaired myotube arrangement within the intrinsic musculature, which was recapitulated in *Shh*$^{+/-}$*; MFCS4*$^{-/+}$ embryos. These results suggest that Shh from the

oropharyngeal epithelium induces the tongue primordium before E10.5 and that subsequent signaling is required for differentiation of the lingual septum during internal lingual muscle patterning (Figure 6).

Our observations from both *CreER^{TM}; Shh$^{flox/flox}$* and *Shh$^{+/-}$; MFCS4$^{-/+}$* mice suggest that myoblast colonization and differentiation are not affected by altered Shh signaling after the initiation of tongue formation, which was further supported by the tongue phenotype associated with *Mesp1-Cre;Ofd$^{fl/Y}$* mice. We found no difference in myogenic cell lineage proliferation patterns between WT and *Shh$^{+/-}$; MFCS4$^{-/+}$* mice, although Shh signaling is often associated with the regulation of cell proliferation (Ulloa and Briscoe, 2007; Xavier et al., 2016; Ertao et al., 2016; Coni et al., 2017). It appears that Shh secreted from the lingual epithelium after the initiation of tongue formation mostly functions to influence tenocyte differentiation within the internal lingual musculature. Although previous studies have suggested that CNC cells are responsible for the initiation of tongue formation through transduction of the Shh signal (Jeong et al., 2004), it is not clear if myoblasts play a role in this event or they are affected by impaired Shh

290 signaling. *Pax3*-positive muscle progenitors initiate migration around E9.75 and reach
291 the pharyngeal region by E11.5 (Relaix et al., 2004). *Wnt1-Cre; Smo*$^{flox/-}$ mice show a
292 cluster of apoptotic cells at the mandibular midline at E9.5, which consequently leads to
293 aglossia. Therefore, it is intriguing to reveal the association between migration of
294 lingual myogenic precursors into the pharyngeal arches and the early stages of tongue
295 formation. There is evidence from studies of TGF-ß signaling during murine tongue
296 formation of a complex interplay between CNC and myogenic precursor cells during
297 this process (Hosokawa et al., 2010; Han et al., 2012; Iwata et al., 2013; Song et al.,
298 2013).
299
300 Removal of *Ofd1* in CNC cells (*Wnt1-Cre; Ofd*$^{fl/Y}$) resulted in a hypoplastic tongue and
301 a complete disruption of myotube arrangement; whereas loss of Smo in CNC cells leads
302 to aglossia (Jeong et al., 2004). The *Ofd1* gene is located on the X-chromosome and
303 encodes a component of the centrosome and basal body of primary cilia, a key mediator
304 of Hedgehog signaling (Satir et al., 2010). Smo is a Hedgehog signal mediator, which
305 facilitates the release of Gli transcription factors from the Hedgehog repressor

306 Suppressor-of-Fused (SuFu). Impaired function of the cilium will result in a variable
307 effect on signal transduction, depending upon the molecular nature (Bang and Anderson,
308 2015) when compared to loss of Smo, which is absolutely required for signal
309 transduction. Mutations in human *OFD1* cause Oral-facial-digital syndrome (OFD) type
310 I, which includes a spectrum of craniofacial phenotypes including gingival frenulae,
311 lingual hamartomas, cleft palate and significantly, a cleft and/or lobulated tongue
312 (reviewed in Franco and Thauvin-Robinet, 2016).
313
314 Tendons represent connective tissues that assemble musculoskeletal tissues and anchor
315 force-generating muscles to the skeleton, which leads to optimal locomotion and
316 mobility in vertebrates. The tendon is required to integrate with muscle and skeleton at
317 the myotendinous junction and enthesis, respectively. The mechanism of tendon
318 formation and attachment has been investigated in the trunk, limb and head (Schweizer
319 et al., 2010; Subramanian et al., 2015). The external tongue muscles originate
320 predominantly from hard tissue outside of the tongue and insert into the tongue dorsum
321 and lingual septum. We have detected diminished expression of Fgfr1 in the

322 lamina propria, future aponeurosis, and lingual septum in the tongue of
323 *Shh*$^{+/-}$; *MFCS4*$^{-/+}$ (Figure 4Q, R). There is evidence that *Scx* expression in the early
324 tongue is dependent upon TGF-ß signaling from CNC cells but not myogenic precursors
325 (Han et al., 2012; Han et al., 2014). The contribution of Shh signaling in tendon
326 formation has been reported in a variety of developmental systems but not the tongue.
327 In chick axis tendon formation, *Shh* expressed from ventral midline structures such as
328 the floor plate and notochord inhibits induction of syndetome which is comprised of
329 tendon progenitor cells. However, Shh indirectly induces *Scx* expression through
330 activation of fibroblast growth factor (FGF) expression in the dermomyotome, which
331 promotes *Scx* transcription in the somite (Brent et al., 2003). In support of this, FGF
332 signaling is required for differentiation of tenocyte precursors in mice (Brent et al.,
333 2005). In the chick digestive system, expression of *Scx* in two tendon domains that
334 develop in close relation to the two visceral smooth muscles also depends upon FGF
335 signaling (Guen et al., 2009) and *Shh* expressed from the endoderm is responsible for
336 inhibition of smooth muscle cell differentiation from the common undifferentiated
337 mesodermal-derived mesenchyme (Sukegawa et al., 2000).A recent study has reported

338 that expression levels of some FGFs are increased during lingual septum formation (Du
339 et al., 2016).Our *ex vivo* organ culture of the tongue with FGF ligand has resulted in
340 successful induction of *Scx*.
341 This concludes that Shh signaling influences tenocyte differentiation through Fgf
342 signaling, but *Sox9* expression without. The interaction between Shh and FGF signaling
343 in tendon formation will require further elucidation to fully understand the molecular
344 mechanisms of tendon development in detail.
345
346 The obstruction of palatal closure by the tongue is widely thought to be a major cause of
347 cleft palate in human populations. One possible cause of this is abnormal muscle
348 formation and function in the tongue. There are suggestive cases reported previously
349 (Iseki et al., 2007; Okano et al., 2012; Song et al., 2013) and the present study also
350 suggests this possibility. It is also speculated that micrognathia results in abnormal
351 placement or development of the tongue, which can lead to cleft palate (reviewed in
352 Price et al., 2016). There is currently no consensus amongst researchers regarding the
353 involvement of the tongue and mandible during secondary palate formation. More

354 evidence will be required to further define this complex relationship amongst these

355 diverse structures during formation of the oro-facial region.

356

Materials and methods

Animals

All animal experiments were performed in accordance with protocols certified by the Institutional Animal Care and Use Committee of King's College London and Tokyo Medical and Dental University. *MFCS4*$^{+/-}$ (Sagai et al., 2009), *Shh*$^{-/+}$ (Amano et al., 2009), *CreER*^{TM} (Hayashi and McMahon, 2002), *Shh*$^{flox/+}$ (Dassule et al., 2000), *Ofd1* (Ferrante et al., 2006), *Wnt1-cre* (Danielian et al., 1997), *Mesp1-cre* (Saga et al., 1999) mice were maintained in a C57BL/6N background. *CreER*^{TM}*; Shh*$^{flox/+}$ mice were mated with *Shh*$^{flox/+}$ mice and pregnant mice received tamoxifen by intraperitoneal injection (75 mg/kg, equivalent to 3 mg per 40g body weight) through the maternal body.

Histological analyses

Specimen were fixed with Bouin's solution for hematoxylin-eosin (H.E.) staining or 4% paraformaldehyde (PFA)/PBS, embedded in paraffin (H.E.) or O.C.T. compound (Sakura Finetek, Tokyo, JP for other histological analyses), and prepared to 5 μm-(paraffin) or 12 μm (frozen)-thick sections. For immunohistochemistry (IHC),

373 anti-desmin antibody (clone D33, 413651, Nichirei Biosciences, Tokyo, JP) at x1
374 dilution, anti-SMA antibody (clone 1A4, A2547-100UL, Sigma, Saint Louis, MO) at
375 x1,000 dilution, anti-BrdU antibody (clone BMC9318, 11 170 376 001, Roche
376 Diagnostics, Basel, CH) at x100 dilution, anti-Myf5 antibody (polyclonal, SAB4501943,
377 Sigma, Saint Louis, MO) at x100 dilution, anti-CD31 antibody (polyclonal, ab28364,
378 Abcam, Cambridge, UK) at x100 dilution, and anti-synaptophysin antibody (clone
379 SY38, ab8049, Abcam, Cambridge, UK) at x100 dilution were used. For visualization,
380 corresponding secondary antibodies, VECTASTAIN ABC Kit (AK-5000, Vectastain,
381 Burlingame, CA) and diaminobenzidine (DAB) were applied, or corresponding
382 fluorescent-conjugated secondary antibody was applied. Hematoxylin and Hoechst
383 33342 were used for counter staining for DAB and fluorescence, respectively.

384 For *in situ* hybridization (ISH), specimens were hybridized with
385 digoxygenin-labeled RNA probes specifically designed complementary to the full- or
386 partial- mRNA of *Shh*, *Ptch1*, *Myf5*, *Sox9*, *Scx*, *Col1a1*, *Fn1*, and *Fgfr1* followed by the
387 incubation with anti-digoxygenin-AP conjugate. Nitro blue tetrazolium chloride (NBT) /
388 5-Bromo-4-chloro-3-indolyl phosphate, toluidine salt (BCIP) were used for

389 colourization. All commercial reagents for ISH were purchased from Roche Diagnostics
390 (Basel, CH). All template DNA for RNA probes were cloned into pTA2 vector (TArget
391 Clone, TAK-101, Toyobo Life Science, Osaka, JP).
392 For X-gal staining (detection of beta-galactosidase), sections were incubated with
393 5-bromo-4-chloro-3-indolyl-β-D-galactoside (X-gal) in phosphate buffer (pH7.3)
394 supplemented with 2 mM $MgCl_2$, 5mM potassium ferrocyanide ($K_4Fe(CN)_6$-$3H_2O$), and
395 5mM potassium ferricyanide ($K_3Fe(CN)_6$) at 37°C after fixation in 4%PFA. Nuclear
396 Fast Red was used for counter staining.
397

398 **Cell proliferation analysis**

399 Sixty minutes before dissection, BrdU at 100mg/ml was injected
400 intraperitoneally to the pregnant mice at 10mg/kg at the designed day. Every 6 of 7
401 sections through the tongue primordium of a specimen were used for cellular
402 proliferation index study. BrdU incorporation and Myf5 localization were detected by
403 immunohistochemistry. Epithelial cells were determined as external cells than the
404 basement membrane by histological observation. Myoblast cell lineage was determined

405 as Myf5-positive cells, and Myf5-negative cells were assumed to be CNC-derived.
406 Proliferation index was calculated by the number of BrdU-positive cells] / [total number
407 of cells of each population] and statistical significance was examined by *t*-test for more
408 than 3 individual experiments for each genotype.
409

410 **Real time RT-PCR**

411 RNA was extracted from the tongue of littermate WT and *Shh*$^{+/-}$; *MFCS4*$^{-/+}$
412 embryos at E12.5 using Direct-zol RNA MiniPrep Kit (R2050S, Zymo Research, Irvine,
413 CA) following the product protocol. 250ng RNA was transcribed to cDNA by ReverTra
414 Ace (TRT-101; Toyobo Life Science, Osaka, JP). Realtime PCR was performed with
415 LightCycler 480 High Resolution Melting Master (04909631001; Roche, Diagnostics,
416 Basel, CH). Normalized to the *actin, beta* gene and relative expression to the littermate
417 WT was shown. Statistical significance was examined by *t*-test for more than 3
418 individual experiments for each genotype.
419

420 **Organ culture**

421 The dissected maxilla (with palatal shelves) of E13.5 *Shh*$^{+/-}$; *MFCS4*$^{-/+}$ or WT
422 littermates were cultured in the mixture of Dulbecco's Modified Eagle's Medium
423 Nutrient Mixture F-12 (Sigma-Aldrich, St. Louis, MO) and BGJb Medium
424 (LifeTechnologies, Grand Island, NY) for 48 hours by supplying 95% O_2 + 5% CO_2 at
425 37°C using rotary culture system.
426 Heparin-coated acrylic beads (diameter, 125–150 mm; Sigma, St Louis, MO) were
427 soaked in either PBS or in 300 mg/mL recombinant human FGF18 (AF-100-28,
428 PEPROTECH, Rocky Hill, NJ) for at least 1 hour at room temperature. The beads were
429 embedded in the tongue with mandible at E11.0 and the tongue underwent the rotary
430 organ culture system as described above for 24 hours.
431

432 **Micro computer tomography images**

433 *Shh*$^{+/-}$; *MFCS4*$^{-/+}$ and their WT littermates at P0 were scanned with X-ray
434 microCT inspeXio SMX-100CT (Shimadzu Corporation, Kyoto, JP) and rendered with
435 VGStudio Max 2.0 (Volume Graphics, Heidelberg, DE). Each figure shown is a

436 representative of more than 3 independent experiments. Pictures paired for comparison

437 were taken and processed under the same condition from the same litter.

438

Acknowledgements

This work was supported by JSPS KAKENHI Grant Numbers 19890071, 22592254, 25463130 and 16K11744 to S.O., and 20390510 to S.I., and NIG-JOINT (2008-A, 2009-B7, 2012-B4) to S.I. H.A.A. was funded by Iraq Higher Committee for Educational Development. K.J.L. received the funding from the BBRSC (Grant BB/I021922/1) and MRC (Grant MR/L017237/1)

S.O. and A.B. are co-first, and M.C. and S.I. are co-corresponding authors.

Figure legends

Figure 1

Temporal loss of Shh function produces graded effects on tongue development.

(A-D) H.E stained frontal histological analysis of the developing tongue in (A) E14.5 WT and (B-D) *CreER^{TM}; Shh$^{fl/fl}$* embryos injected with tamoxifen at E10.5, E11.5, E12.5 and harvested 3 days later, respectively; (E-H) Highlight of intrinsic muscle organization in the tongue dorsum identified within the black rectangles (A-D); (I-P) ISH of *Myod1* (I-L) and *Scx* (M-P) on WT (I, M), and *CreER^{TM}; Shh$^{fl/fl}$* embryos that received tamoxifen at E10.5, E11.5, E12.5 and were harvested 3 days later (J, N; K, O; L, P; respectively). *Scx* expression in WT embryos at E14.5 is highlighted in (M) in the lingual septum (arrow), genioglossus (small arrowhead) and geniohyoid (large arrowhead) muscles. Scale bar in P=100µm for A-D and I-P; in H=100µm for E-H.

460 **Figure 2**

461 **Reduced Shh signaling in the lingual epithelium results in impaired**

462 **myotube arrangement and tendon formation.**

463 (A-D) ISH for *Shh* (A, B) and *Ptch1* (C, D) on sagittal sections of WT littermate (A,

464 C) and *Shh*$^{+/-}$*; MFCS4*$^{-/+}$ (B, D) heads at E11.5. (E) Semi-quantitative RT-PCR analysis

465 of *Shh*, *Ptch1*, and *Myf5* transcription in the tongue of the *Shh*$^{+/-}$*; MFCS4*$^{-/+}$ and the

466 littermate WT at E12.5. (F, G) Myoblast immigration was analyzed by ISH of *Myf5* (F,

467 G) on sagittal sections of E11.5 WT (F) and *Shh*$^{+/-}$*; MFCS4*$^{-/+}$ (G) head. The anterior is

468 to the left. (H-K) Myoblast differentiation was investigated by ISH of *Myod1* (H, I) and

469 IHC of desmin (J, K) at anterior (Ha, Ia, Ja, Ka) and posterior (Hp, Ip, Jp, Kp) region on

470 coronal sections of E11.5 WT (H, J) and *Shh*$^{+/-}$*; MFCS4*$^{-/+}$ (G). The level of the section

471 obtained was indicated as a for the anterior and p for the posterior in F. (L-O) ISH of

472 *Myod1* and *Scx* on coronal section of E13.5 WT (L, N) and *Shh*$^{+/-}$*; MFCS4*$^{-/+}$ (M, O).

473 Arrowheads indicate the short tendon of genioglossus origin at the superior mental

474 spine. The line of the future aponeurosis is drawn as the dotted line in N, which is not

475 consecutive in the *Shh*$^{+/-}$*; MFCS4*$^{-/+}$ (arrows in O). Lingual septum in the litte

476 rmate WT was indicated double arrows in N. m; mandible, t; tongue, sl; superior

477 longitudinal muscle, vt; vertical and transverse muscle, sg; styloglossus. Scale bar for

478 A-K is in G. Scale bar for L-O is in O.

479

480 **Figure 3**

481 **Shh signaling is received by CNC cells for tendon formation and myotube**

482 **arrangement.**

483 (A-C) Lingual CNC-derived mesenchyme was visualized by X-gal staining on frontal

484 (A) and sagittal (B, C) sections of *Wnt1cre; R26R* at E12.5. C is a magnified view of the

485 boxed area in B. (D, E) Shh signal receiving cells were determined by ISH of *Ptch1* (D)

486 and *Myf5* (E) on adjacent sections to B and corresponding region to C. Arrows indicate

487 superior longitudinal muscles in C, D, E. (F-K) The levels of Shh signal is studied by

488 *Ptch1* ISH on sagittal sections of E11.5 (F-H) and E12.5 (I-K) WT (F, I), *Wnt1-Cre;*

489 $Ofd^{fl/Y}$ (G, J) and *Mesp1-Cre;* $Ofd^{fl/Y}$ (H, K). (L-N) Lingual myotube arrangement is

490 examined by *Myod1* ISH on coronal sections of E13.5 WT (L), *Wnt1-Cre;* $Ofd^{fl/Y}$ (M)

491 and *Mesp1-Cre;* $Ofd^{fl/Y}$ (N). m; is mandibular process, t; tongue, ht; heart, ps; palatal

492 shelf.

493

Figure 4

Shh signaling is responsible for differentiation of lingual CNC cells.

(A-F) Detection of a mesenchymal marker *Sox9* transcripts on coronal sections at E11.75 (A, B), 12.75 (C, D) and 13.75 (E, F) in WT (A, C, E) and the *Shh*$^{+/-}$*; MFCS4*$^{-/+}$ (B, D, F). *Sox9* expression in the future lingual septum is indicated by arrow in C. (G-L) Stage specific expression of *Scx* was detected on coronal sections of the tongue by ISH (G-J) and whole mount ISH (K, L) at E11.75 (G, H) and E12.75 (I-L) in WT (G, I, K) and *Shh*$^{+/-}$*; MFCS4*$^{-/+}$ (H, J, L). The expression in the future aponeurosis and the lingual septum is indicated by arrows and the dotted line. (M-R) Lingual mesenchyme differentiation was investigated by ISH of *Col1a1* (M, N), *Fn1* (O, P), and *Fgfr1* (Q, R) and IHC of desmin (S, T) on coronal sections of the WT (M, O, Q, S) and *Shh*$^{+/-}$*; MFCS4*$^{-/+}$ (N, P, R, T). (Y) Lingual CNC-derived and mesoderm-derived mesenchymal cell proliferation index was analyzed at E11.75 and E12.75 in WT and *Shh*$^{+/-}$*; MFCS4*$^{-/+}$. gg; genioglossus muscle. (U-X) E11.0 Mandible after 24h organ culture with FGF18- or PBS-soaked beads were subjected to ISH for *Sox9* and *Scx*. Ectopic expression in the mesenchyme and enhanced expression of *Scx* in genioglossus muscle (arrowheads)

were found in the tongue with FGF18 (U). Sox9 expression was not altered by FGF ligand application (W, X). b; beads, m; Meckel's cartilage.

513 **Figure 5**

514 **Abnormal tongue formation induces cleft palate.**

515 (A-F) H.E staining on frontal sections of WT (A, C, E) and *Shh*$^{+/-}$*; MFCS4*$^{-/+}$ (B, D, F)

516 embryos at E13.25 (A, B), E14.0 (C, D) and E14.5 (E, F). (G, H) Aboral view of the

517 secondary palate after organ culture of E13.5 maxilla of WT (G) and *Shh*$^{+/-}$*; MFCS4*$^{-/+}$

518 (H). ps; palatal shelf, t; tongue

519

520 **Figure 6**

521 **Schematic representation of Shh signaling from the oropharyngeal**

522 **epithelium during tongue development.**

523 The embryonic stage colored in red requires Shh synthesized in the oropharyngeal

524 epithelium. Shh influences CNC-derived mesenchyme (pink) to initiate tongue

525 development and lingual tendon formation during the arrangement of intrinsic lingual

526 muscles.

527

Figure Supplement 1

Vascularization and innervation is not affected in *Shh*$^{+/-}$; *MFCS4*$^{-/+}$.

(A, B) Immunofluorescent detection of an endothelial marker CD31 (green) on E13.5 coronal sections of WT (A) and *Shh*$^{+/-}$; *MFCS4*$^{-/+}$ (B). (C, D) Immunofluorescent detection of the neuron marker synaptophysin (green) on E13.5 coronal sections of WT (C) and *Shh*$^{+/-}$; *MFCS4*$^{-/+}$ (D). Nuclei are stained blue by Hoechest. Both vascular endothelial cells (A, B) and pre-synaptic protein (C, D) were detected in a similar manner in WT and *Shh*$^{+/-}$; *MFCS4*$^{-/+}$.

537 **Figure Supplement 2**

538 ***Shh*$^{+/-}$*; MFCS4*$^{-/+}$ **mice exhibit cleft palate and disorganized myotube**

539 **arrangement at P0.**

540 (A-D) Maxillae (A, B) and mandibles (C, D) of WT (A, C) and *Shh*$^{+/-}$*; MFCS4*$^{-/+}$ (C,

541 D). **WT** palate is fully fused in the midline whereas that of *Shh*$^{+/-}$*; MFCS4*$^{-/+}$ is

542 completely cleft (asterisk). Double-headed arrow points the soft palate region and the

543 number is given to each ruga. The *Shh*$^{+/-}$*; MFCS4*$^{-/+}$ also demonstrate short soft palate.

544 The size of the mandible of *Shh*$^{+/-}$*; MFCS4*$^{-/+}$ is similar to that of WT. The tongue has

545 been distorted with grooves that are considered to be the impression by the palatal

546 shelves (arrowheads). *Shh*$^{+/-}$*; MFCS4*$^{-/+}$ exhibit disorganized myotubes arrangement.

547 (E-H) Immunofluorescent detection of a myotube marker smooth muscle actin (SMA)

548 on coronal sections of WT (E) and *Shh*$^{+/-}$*; MFCS4*$^{-/+}$ (F). G and H are magnified views

549 of the boxed area in E and F, respectively. Myotube arrangement in WT was symmetric

550 and both vertical and transverse myotubes are arranged in order. In contrast, *Shh*$^{+/-}$*;*

551 *MFCS4*$^{-/+}$ myotube arrangement is asymmetric and disturbed, especially in the midline

552 area due to lack of lingual septum formation.

553

554 **Figure supplement 3**

555 **Skeletal defects in *Shh*$^{+/-}$; *MFCS4*$^{-/+}$.**

556 MicroCT scanned maxilla (A-C), posterior cranial base (D-F), profile (G-I), and

557 skeleton cut at midline (H-J) of *Shh*$^{+/-}$; *MFCS4*$^{-/+}$ and the wild type at P0. The *Shh*$^{+/-}$;

558 *MFCS4*$^{-/+}$ with severe phenotype (B, E, H, L) and milder phenotype (C, F, I, K) are

559 shown to be compared with the wild type (A, D, G, J).

560 Smaller or missing prepalatal bone and vomer, premaxilla, basis of sphenoid bone were

561 found in the *Shh*$^{+/-}$; *MFCS4*$^{-/+}$ (A-F, J-L). Hyoid bone and tympanic ring of the *Shh*$^{+/-}$;

562 *MFCS4*$^{-/+}$ were also smaller than those of the wild type. Basoccipital bones of the

563 *Shh*$^{+/-}$; *MFCS4*$^{-/+}$ had a notch at anterior edge where derived from CNC cells (D-F).

564 These phenotypes met with the origin of each bone and active region of MFCS4.

565 Prepalatal bone and vomer; yellow, premaxilla; cyan, sphenoid bone; magenta,

566 basoccipital bone; green, hyoid bone; red, tympanic ring; blue. Lateral view is the

567 merge of skeletal system with soft tissue in grey.

568

569

References

1. Micrognathia in mouse models of ciliopathies

H Adel Al-Lami, WB Barrell, KJ Liu (2016)

Biochemical Society Transactions **44**:1753-1759.

https://doi.org/10.1042/BST20160241

2. Sox9 is required for determination of the chondrogenic cell lineage in the cranial neural crest

Y Mori-Akiyama, H Akiyama, DH Rowitch, B de Crombrugghe (2003)

PNAS **100**:9360-9365.

https://doi.org/10.1073/pnas.1631288100

3. Chromosomal dynamics at the Shh locus: limb bud-specific differential regulation of competence and active transcription

T Amano, T Sagai, H Tanabe, Y Mizushina, H Nakazawa, T Shiroishi (2009)

Developmental Cell **16**:47-57.

https://doi.org/10.1016/j.devcel.2008.11.011

4. Lineage specificity of primary cilia in the mouse embryo

FK Bangs, N Schrode, AK Hadjantonakis, KV Anderson (2015)

Nature Cell Biology **17**:113-122

https://doi.org/10.1038/ncb3091

5. Sonic hedgehog from pharyngeal arch 1 epithelium is necessary for early mandibular arch cell survival and later cartilage condensation differentiation

KK Billmyre, J Klingensmith (2015)

Developmental Dynamics **244**:564-576.

https://doi.org/10.1002/dvdy.24256

6. A somitic compartment of tendon progenitors

AE Brent, R Schweitzer, CJ Tabin (2003)

Cell **113**:235-248.

7. Genetic analysis of interactions between the somitic muscle, cartilage and tendon cell lineages during mouse development

AE Brent, T Braun, CJ Tabin (2005)

Development **132**:515-528.

https://doi.org/10.1242/dev.01605

8. Craniofacial ciliopathies reveal specific requirements for GLI proteins during development of the facial midline

CF Chang, YT Chang, G Millington, SA Brugmann (2016)

PLoS Genetics **12**:e1006351.

https://doi.org/10.1371/journal.pgen.1006351

9. Cyclopia and defective axial patterning in mice lacking Sonic hedgehog gene function

618 C Chiang, Y Litingtung, E Lee, KE Young, JL Corden, H Westphal, PA Beachy

619 (1996)

620 *Nature* **383**:407-413.

621 https://doi.org/10.1038/383407a0

622

623 10. Selective targeting of HDAC1/2 elicits anticancer effects through Gli1 acetylation in

624 preclinical models of SHH Medulloblastoma

625 S Coni, AB Mancuso, L Di Magno, G Sdruscia, S Manni, SM Serrao, D Rotili, E

626 Spiombi, F Bufalieri, M Petroni, M Kusio-Kobialka, E De Smaele, E Ferretti, C

627 Capalbo, A Mai, P Niewiadomski, I Screpanti, L Di Marcotullio, G Canettieri

628 (2017)

629 *Scientific Reports* 7:44079.

630 https://doi.org/10.1038/srep44079

631

632 11. A 5.5-kb enhancer is both necessary and sufficient for regulation of Wnt-1

633 transcription in vivo

PS Danielian, Y Echelard, G Vassileva, AP McMahon (1997)

Developmental Biology **192**:300-309.

https://doi.org/10.1006/dbio.1997.8762

12. Sonic hedgehog regulates growth and morphogenesis of the tooth

HR Dassule, P Lewis, M Bei, R Maas, AP McMahon (2000)

Development **127**:4775-4785.

13. Expression of FGFs during early mouse tongue development

W Du, J Prochazka, M Prochazkova, OD Klein (2016)

Gene Expression Patterns **20**:81-87.

https://doi.org/10.1016/j.gep.2015.12.003

14. Autocrine Sonic hedgehog signaling promotes gastric cancer proliferation through induction of phospholipase Cγ1 and the ERK1/2 pathway

Z Ertao, C Jianhui, C Chuangqi, Q Changjiang, C Sile, H Yulong, W Hui, C

650 Shirong (2016)

651 *Journal of Experimental & Clinical Cancer Research* **35**:63.

652 https://doi.org/10.1186/s13046-016-0336-9

653

654 15. Oral-facial-digital type I protein is required for primary cilia formation and

655 left-right axis specification

656 MI Ferrante, A Zullo, A Barra, S Bimonte, N Messaddeq, M Studer, P Dollé, B

657 Franco (2006)

658 *Nature Genetics* **38**:112-117.

659 https://doi.org/10.1038/ng1684

660

661 16. Update on oral-facial-digital syndromes (OFDS).

662 B Franco, C Thauvin-Robinet (2016)

663 *Cilia* **5**:12.

664 https://doi.org/10.1186/s13630-016-0034-4

665

17. The role of the sonic hedgehog signalling pathway in patients with midline defects and congenital hypopituitarism

LC Gregory, C Gaston-Massuet, CL Andoniadou, G Carreno, EA Webb, D Kelberman, MJ McCabe, L Panagiotakopoulos, JW Saldanha, HA Spoudeas, J Torpiano, M Rossi, J Raine, N Canham, JP Martinez-Barbera, MT Dattani (2015)

Clinical Endocrinology **82**:728-738.

https://doi.org/10.1111/cen.12637

18. Intermuscular tendons are essential for the development of vertebrate stomach

L Le Guen, C Notarnicola, P de Santa Barbara (2009)

Development **136**:791-801.

https://doi.org/10.1242/dev.029942

19. A TGFß-Smad4-Fgf6 signaling cascade controls myogenic differentiation and myoblast fusion during tongue development

D Han, H Zhao, C Parada, JG Hacia, P Jr Bringas, Y Chai (2012)

Development **139**:1640-1650.

20. ALK5-mediated transforming growth factor ß signaling in neural crest cells controls craniofacial muscle development via tissue-tissue interactions
A Han, H Zhao, J Li, R Pelikan, Y Chai (2014)
Molecular and Cellular Biology **34**:3120-3131.
https://doi.org/10.1128/MCB.00623-14

21. Efficient recombination in diverse tissues by a tamoxifen-inducible form of Cre: a tool for temporally regulated gene activation/inactivation in the mouse
S Hayashi, AP McMahon (2002)
Developmental Biology **244**:305-318.
https://doi.org/10.1006/dbio.2002.0597

22. TGF-beta mediated FGF10 signaling in cranial neural crest cells controls development of myogenic progenitor cells through tissue-tissue interactions during

tongue morphogenesis

R Hosokawa, K Oka, T Yamaza, J Iwata, M Urata, X Xu, P Jr Bringas, K Nonaka, Y Chai (2010)

Developmental Biology **341**:186-195.

https://doi.org/10.1016/j.ydbio.2010.02.030

23. Experimental induction of palate shelf elevation in glutamate decarboxylase 67-deficient mice with cleft palate due to vertically oriented palatal shelf

S Iseki, M Ishii-Suzuki, N Tsunekawa, Y Yamada, K Eto, K Obata (2007)

Birth Defects Research. Part A, Clinical And Molecular Teratology **79**:688-695.

https://doi.org/10.1002/bdra.20400

24. Noncanonical transforming growth factor ß (TGFß) signaling in cranial neural crest cells causes tongue muscle developmental defects

J Iwata, A Suzuki, RC Pelikan, TV Ho, Y Chai (2013)

The Journal of Biological Chemistry **288**:29760-29770.

https://doi.org/10.1074/jbc.M113.493551

25. Hedgehog signaling in the neural crest cells regulates the patterning and growth of facial primordia

J Jeong, J Mao, T Tenzen, AH Kottmann, AP McMahon (2004)

Genes & Development **18**:937-951.

https://doi.org/10.1101/gad.1190304

26. Shh, Bmp-2, Bmp-4 and Fgf-8 are associated with initiation and patterning of mouse tongue papillae

HS Jung, V Oropeza, I Thesleff (1999)

Mechanisms of Development **81**:179-182.

27. Embryonic expression of an Nkx2-5/Cre gene using ROSA26 reporter mice

KA Moses, F DeMayo, RM Braun, JL Reecy, RJ Schwartz (2001)

Genesis **31**:176-180.

28. The differentiation and morphogenesis of craniofacial muscles

DM Noden, P Francis-West (2006)

Developmental Dynamics **235**:1194-1218.

https://doi.org/10.1002/dvdy.20697

29. The regulation of endogenous retinoic acid level through CYP26B1 is required for elevation of palatal shelves

J Okano, W Kimura, VE Papaionnou, N Miura, G Yamada, K Shiota, Y Sakai (2012)

Developmental Dynamics **241**:1744-1756.

https://doi.org/10.1002/dvdy.23862

30. Molecular and cellular regulatory mechanisms of tongue myogenesis

C Parada, D Han, Y Chai (2012)

Journal of Dental Research **91**:528-535.

https://doi.org/10.1177/0022034511434055

31. Disruption of the ERK/MAPK pathway in neural crest cells as a potential cause of Pierre Robin sequence
C Parada, D Han, A Grimaldi, P Sarrión, SS Park, R Pelikan, PA Sanchez-Lara, Y Chai (2015)
Development **142**:3734-3745.
https://doi.org/10.1242/dev.125328

32. Hedgehog signaling in prostate epithelial-mesenchymal growth regulation
YC Peng, AL Joyner (2015)
Developmental Biology **400**:94-104.
https://doi.org/10.1016/j.ydbio.2015.01.019

33. Analysis of the Relationship Between Micrognathia and Cleft Palate: A Systematic Review

762 KE Price, Y Haddad, WD Fakhouri (2016)

763 *The Cleft Palate-Craniofacial Journal* **53**:e34-44.

764 https://doi.org/10.1597/14-238

765

766 34. Divergent functions of murine Pax3 and Pax7 in limb muscle development

767 F Relaix, D Rocancourt, A Mansouri, M Buckingham (2004)

768 *Genes & Development* **18**:1088-1105.

769

770 35. MesP1 is expressed in the heart precursor cells and required for the formation of a

771 single heart tube

772 Y Saga, S Miyagawa-Tomita, A Takagi, S Kitajima, Ji Miyazaki, T Inoue (1999)

773 *Development* **126**:3437-3447.

774

775 36. A cluster of three long-range enhancers directs regional Shh expression in the

776 epithelial linings

777 T Sagai, T Amano, M Tamura, Y Mizushina, K Sumiyama, T Shiroishi (2009)

Development **136**:1665-1674.

https://doi.org/10.1242/dev.032714

37. The primary cilium at a glance

P Satir, LB Pedersen, ST Christensen (2010)

Journal of Cell Science **123**:499-503

https://doi.org/10.1242/jcs.050377

38. Analysis of the tendon cell fate using Scleraxis, a specific marker for tendons and ligaments

R Schweitzer, JH Chyung, LC Murtaugh, AE Brent, V Rosen, EN Olson, A Lassar, CJ Tabin (2001)

Development **128**:3855-3866.

39. Connecting muscles to tendons: tendons and musculoskeletal development in flies and vertebrates

794 R Schweitzer, E Zelzer, T Volk (2010)

795 *Development* **137**: 2807-2817.

796 https://doi.org/10.1242/dev.047498

797

798 40. Mice with Tak1 deficiency in neural crest lineage exhibit cleft palate associated

799 with abnormal tongue development

800 Z Song, C Liu, J Iwata, S Gu, A Suzuki, C Sun, W He, R Shu, L Li, Y Chai, Y Chen

801 (2013)

802 *The Journal of Biological Chemistry* **288**:10440-10450.

803 https://doi.org/10.1074/jbc.M112.432286

804

805 41. The transcription factor Sox9 is required for cranial neural crest development in

806 Xenopus

807 RF Spokony, Y Aoki, N Saint-Germain, E Magner-Fink, JP Saint-Jeannet (2002)

808 *Development* **129**:421-432.

809

42. Tendon development and musculoskeletal assembly: emerging roles for the extracellular matrix
A Subramanian, TF Schilling (2015)
Development **142**:4191-4204.
https://doi.org/10.1242/dev.114777

43. The concentric structure of the developing gut is regulated by Sonic hedgehog derived from endodermal epithelium
A Sukegawa, T Narita, T Kameda, K Saitoh, T Nohno, H Iba, S Yasugi, K Fukuda (2000)
Development **127**:1971-1980.

44. $Scx^+/Sox9^+$ progenitors contribute to the establishment of the junction between cartilage and tendon/ligament
Y Sugimoto, A Takimoto, H Akiyama, R Kist, G Scherer, T Nakamura, Y Hiraki, C Shukunami (2013)

826 *Development* **140**: 2280-2288.

827 https://doi.org/10.1242/dev.096354

828

829 45. A novel ciliopathic skull defect arising from excess neural crest

830 JM Tabler, CP Rice, KJ Liu, JB Wallingford (2016)

831 *Developmental Biology* **417**:4-10.

832 https://doi.org/10.1016/j.ydbio.2016.07.001

833

834 46. Signalling networks regulating dental development

835 I Thesleff, P Sharpe (1997)

836 *Mechanisms of Development* **67**:111-123.

837

838 47. Morphogens and the control of cell proliferation and patterning in the spinal cord

839 F Ulloa, J Briscoe (2007)

840 *Cell Cycle* **6**:2640-2649.

841 https://doi.org/10.4161/cc.6.21.4822

842

843 48. Hedgehog receptor function during craniofacial development

844 GM Xavier, M Seppala, W Barrell, AA Birjandi, F Geoghegan, MT Cobourne (2016)

845 *Developmental Biology* **415**:198-215.

846 https://doi.org/10.1016/j.ydbio.2016.02.009

847

848 49. Next generation limb development and evolution: old questions, new perspectives

849 A Zuniga (2015)

850 *Development* **142**:3810-3820.

851 https://doi.org/10.1242/dev.125757

852

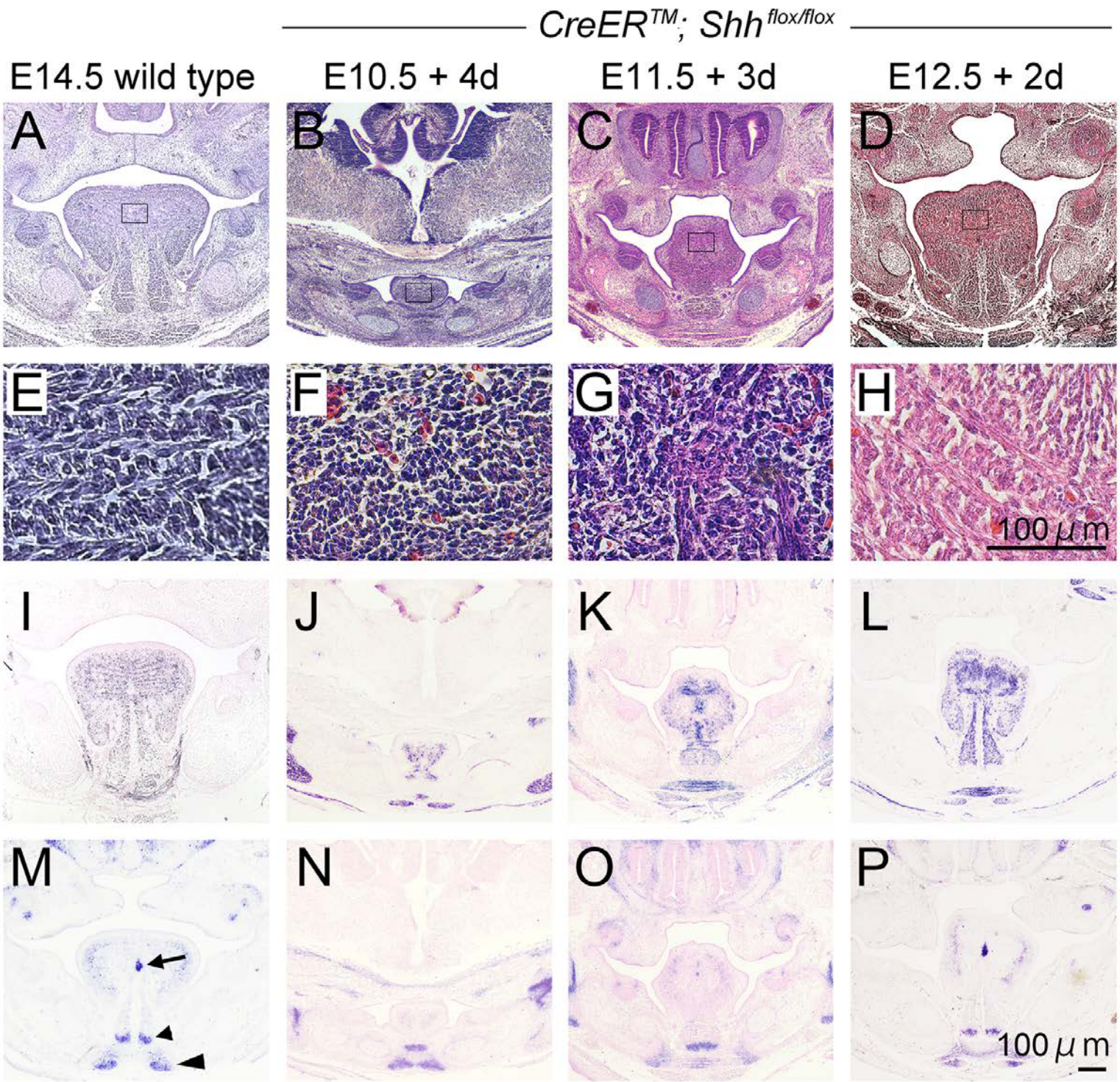
CreER™; Shh flox/flox
E14.5 wild type
E10.5 + 4d
E11.5 + 3d
E12.5 + 2d
H.E
H.E
Myod1
Scx
A
B
C
D
E
F
G
H
I
J
K
L
M
N
O
P
100 μm
100 μm

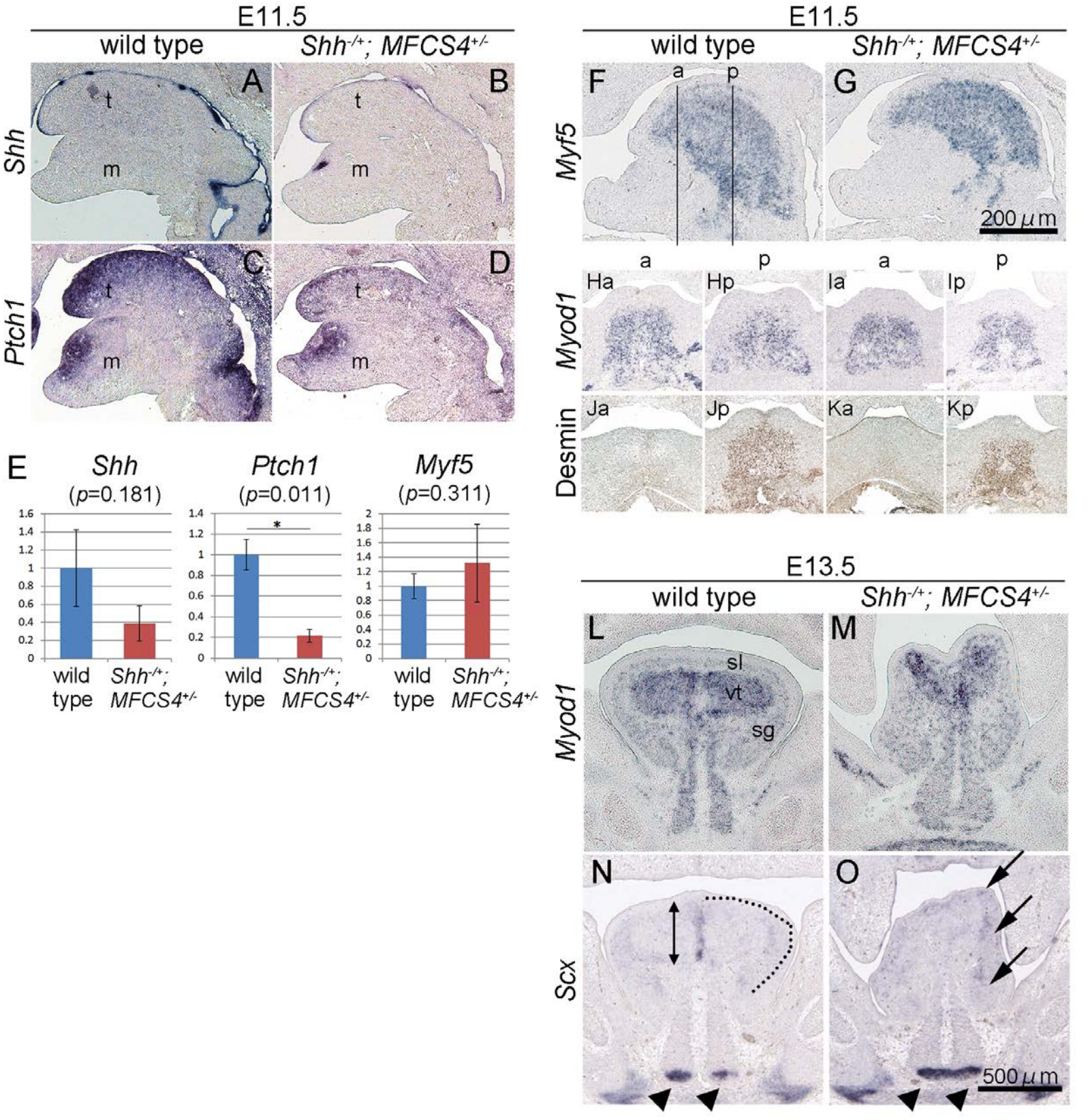
E11.5
wild type
Shh-/+; MFCS4+/-
Shh
Ptch1
A
B
C
D
t
m
E
Shh
(p=0.181)
Ptch1
(p=0.011)
Myf5
(p=0.311)
*
wild type
Shh-/+; MFCS4+/-
E11.5
wild type
Shh-/+; MFCS4+/-
Myf5
Myod1
Desmin
F
G
a
p
200 μm
Ha
Hp
Ia
Ip
Ja
Jp
Ka
Kp
E13.5
wild type
Shh-/+; MFCS4+/-
Myod1
Scx
L
M
N
O
sl
vt
sg
500 μm

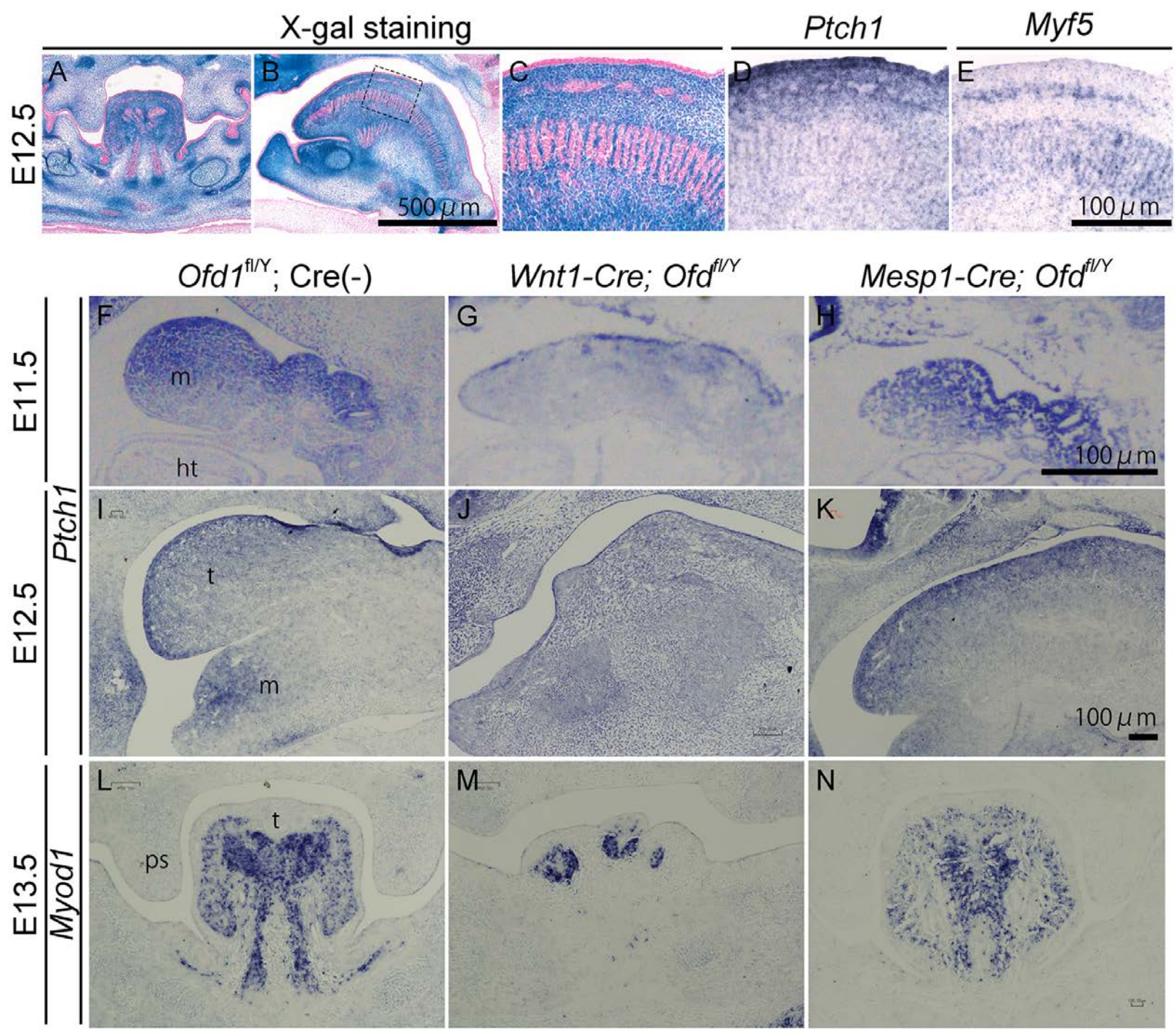
X-gal staining
Ptch1
Myf5
E12.5
A
B
C
D
E
500 μm
100 μm
Ofd1fl/Y; Cre(-)
Wnt1-Cre; Ofdfl/Y
Mesp1-Cre; Ofdfl/Y
E11.5
Ptch1
E12.5
E13.5
Myod1
F
G
H
I
J
K
L
M
N
m
ht
t
ps
100 μm
100 μm

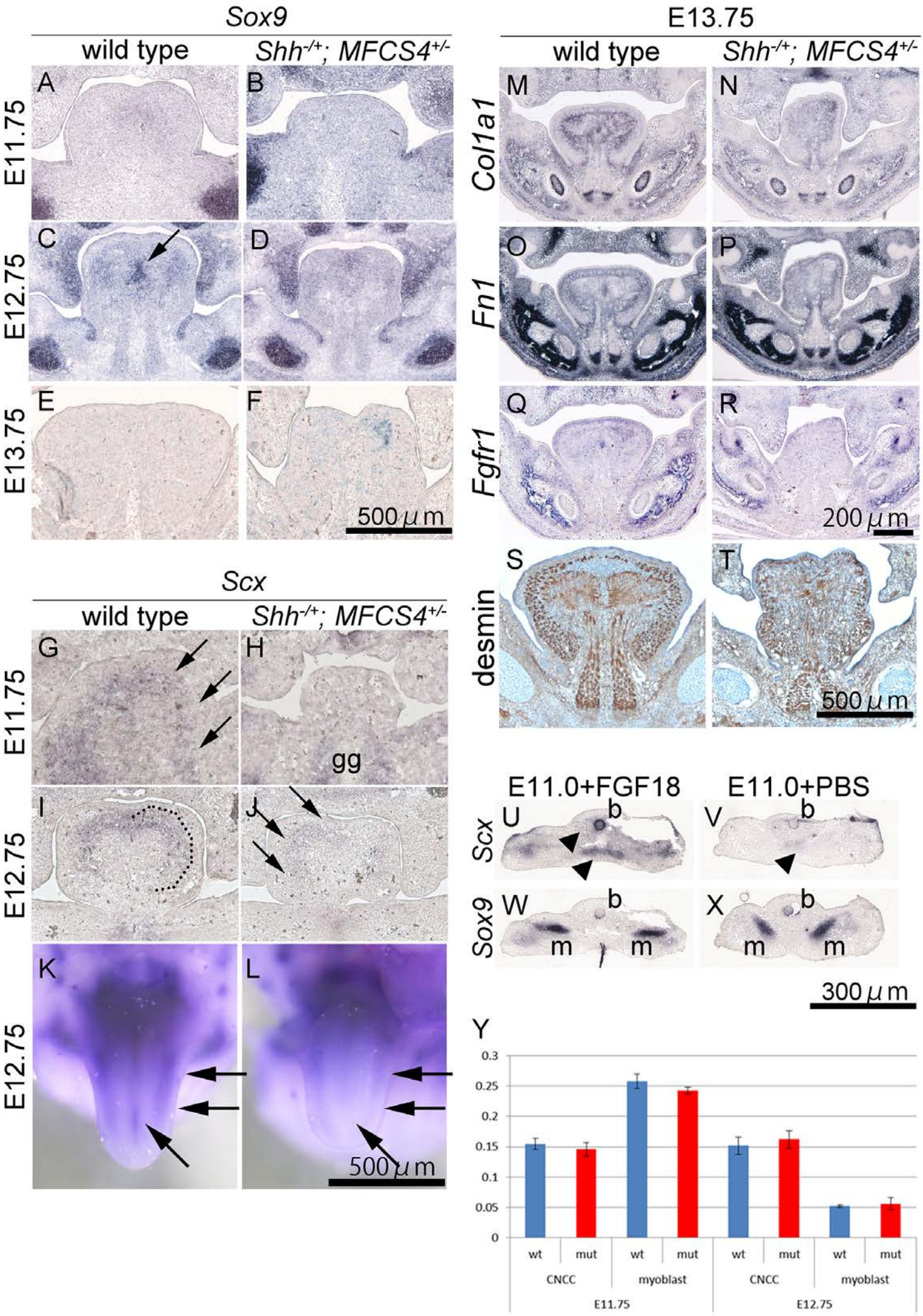
Sox9
wild type
Shh-/+; MFCS4+/-
E11.75
E12.75
E13.75
A
B
C
D
E
F
500 μm
Scx
G
H
gg
I
J
K
L
E13.75
wild type
Shh-/+; MFCS4+/-
Col1a1
Fn1
Fgfr1
desmin
M
N
O
P
Q
R
S
T
200 μm
500 μm
E11.0+FGF18
E11.0+PBS
Scx
Sox9
U
V
W
X
b
m
300 μm
Y
0.3
0.25
0.2
0.15
0.1
0.05
0
wt
mut
CNCC
myoblast
E11.75
E12.75

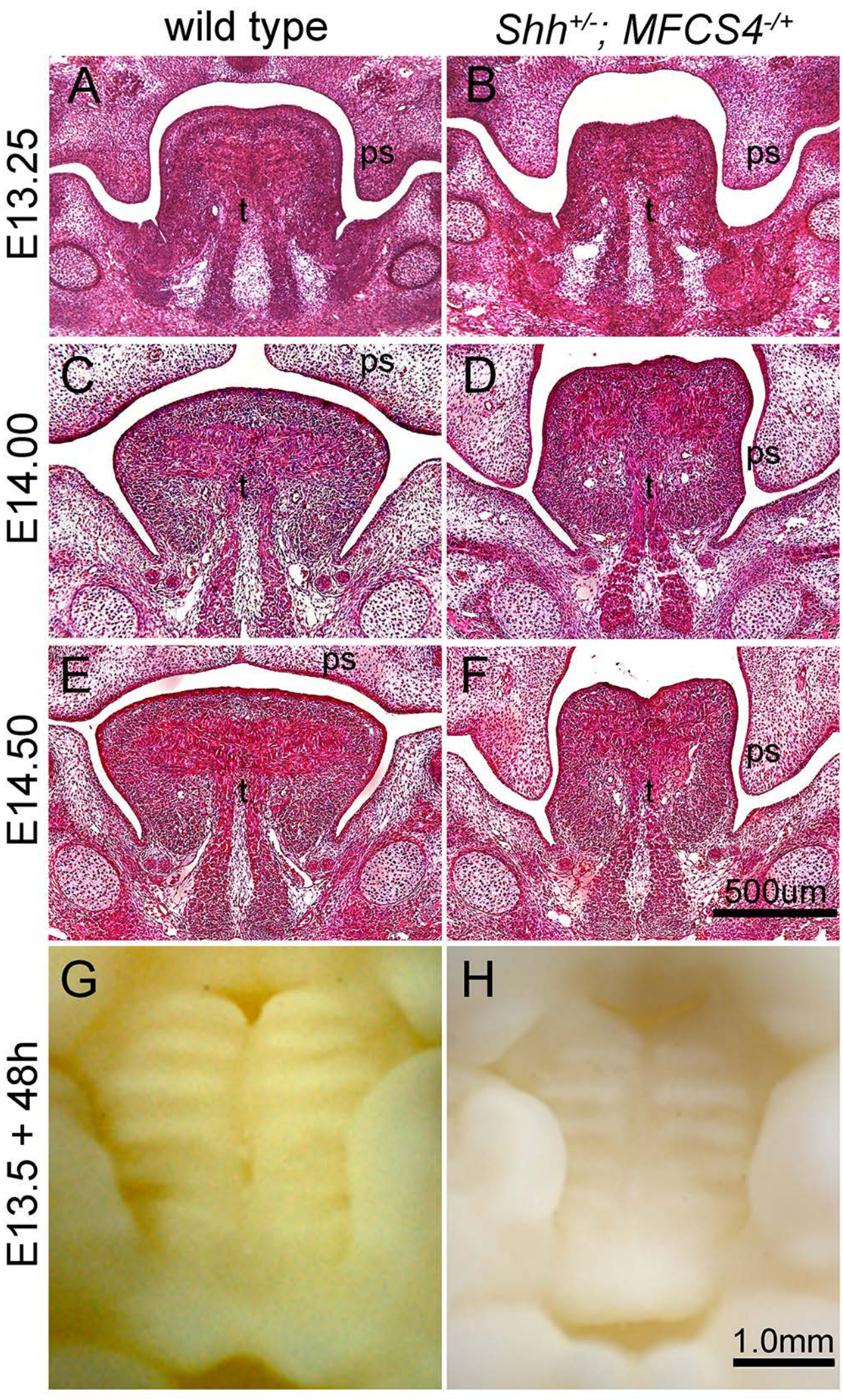
wild type
Shh+/-; MFCS4-/+
E13.25
E14.00
E14.50
E13.5 + 48h
A
B
C
D
E
F
G
H
ps
t
500um
1.0mm

Shh from the epithelium

CNC cell

myoblast precursor

E8.5

E9.5

E10.5

E11.5

E12.5

PA mesenchyme

migration

tongue mesenchyme

tendon differentiation

colonization differntiation

arrangement

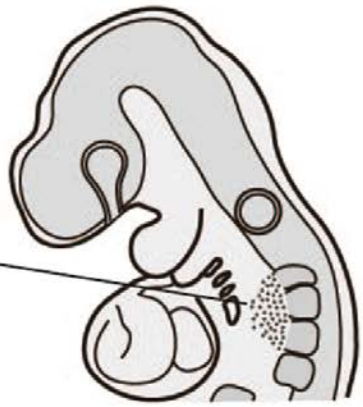

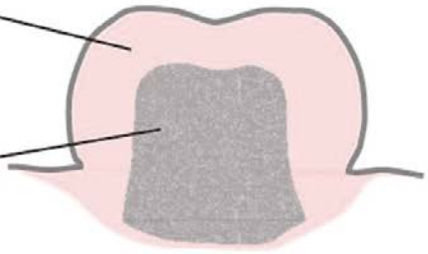

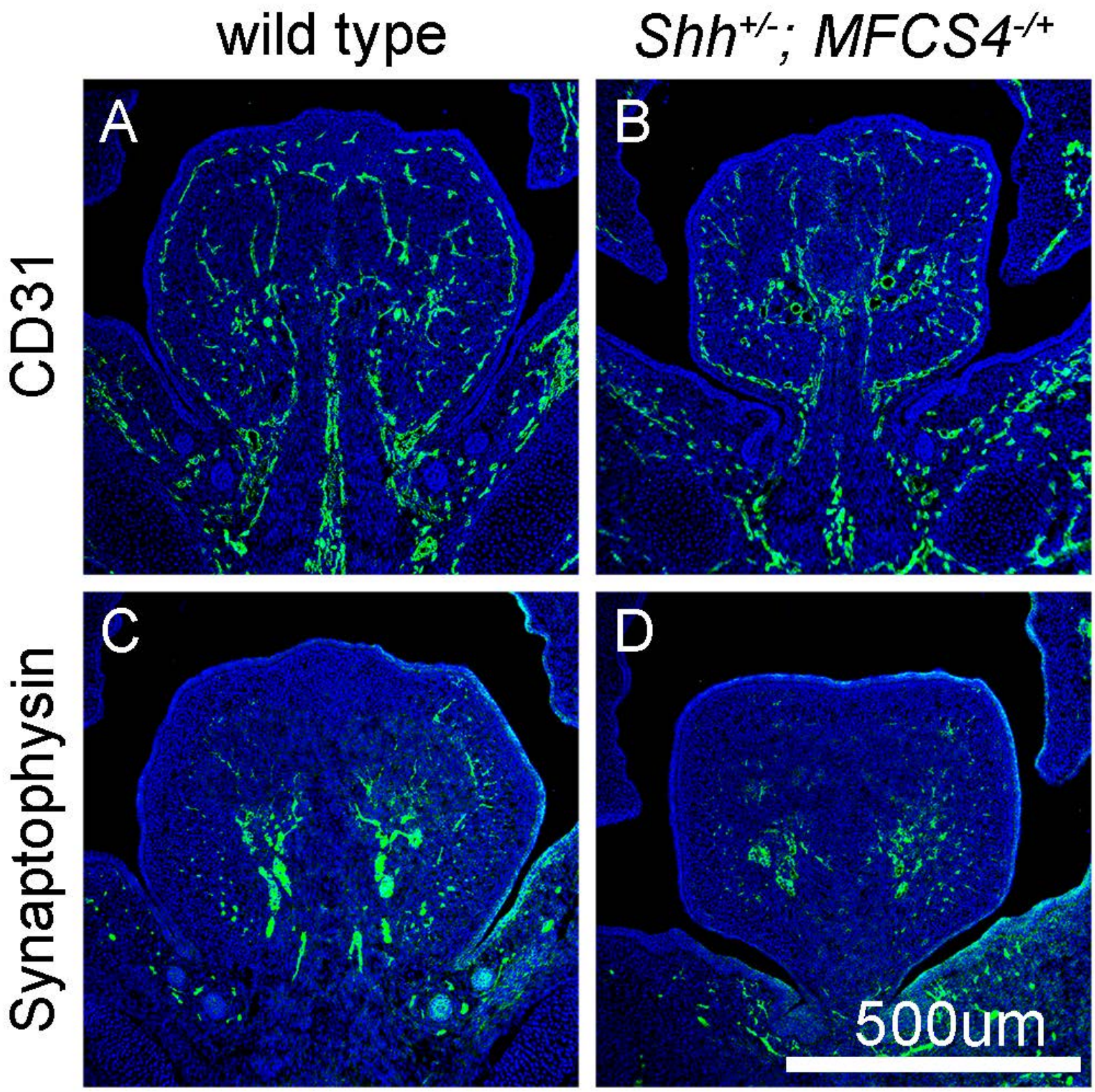
wild type
Shh+/-; MFCS4-/+
CD31
Synaptophysin
A
B
C
D
500um

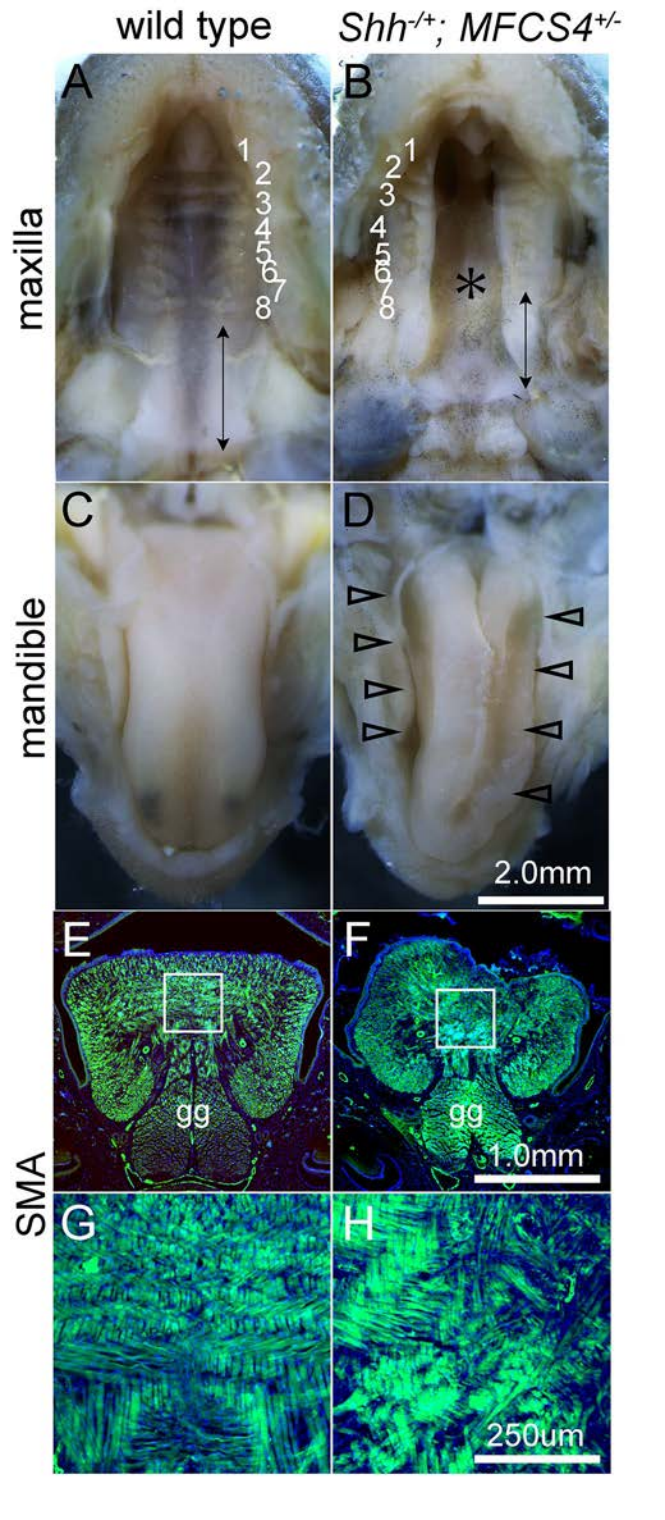
wild type
Shh-/+; MFCS4+/-
maxilla
mandible
SMA
A
B
C
D
E
F
G
H
1
2
3
4
5
6
7
8
*
gg
gg
2.0mm
1.0mm
250um

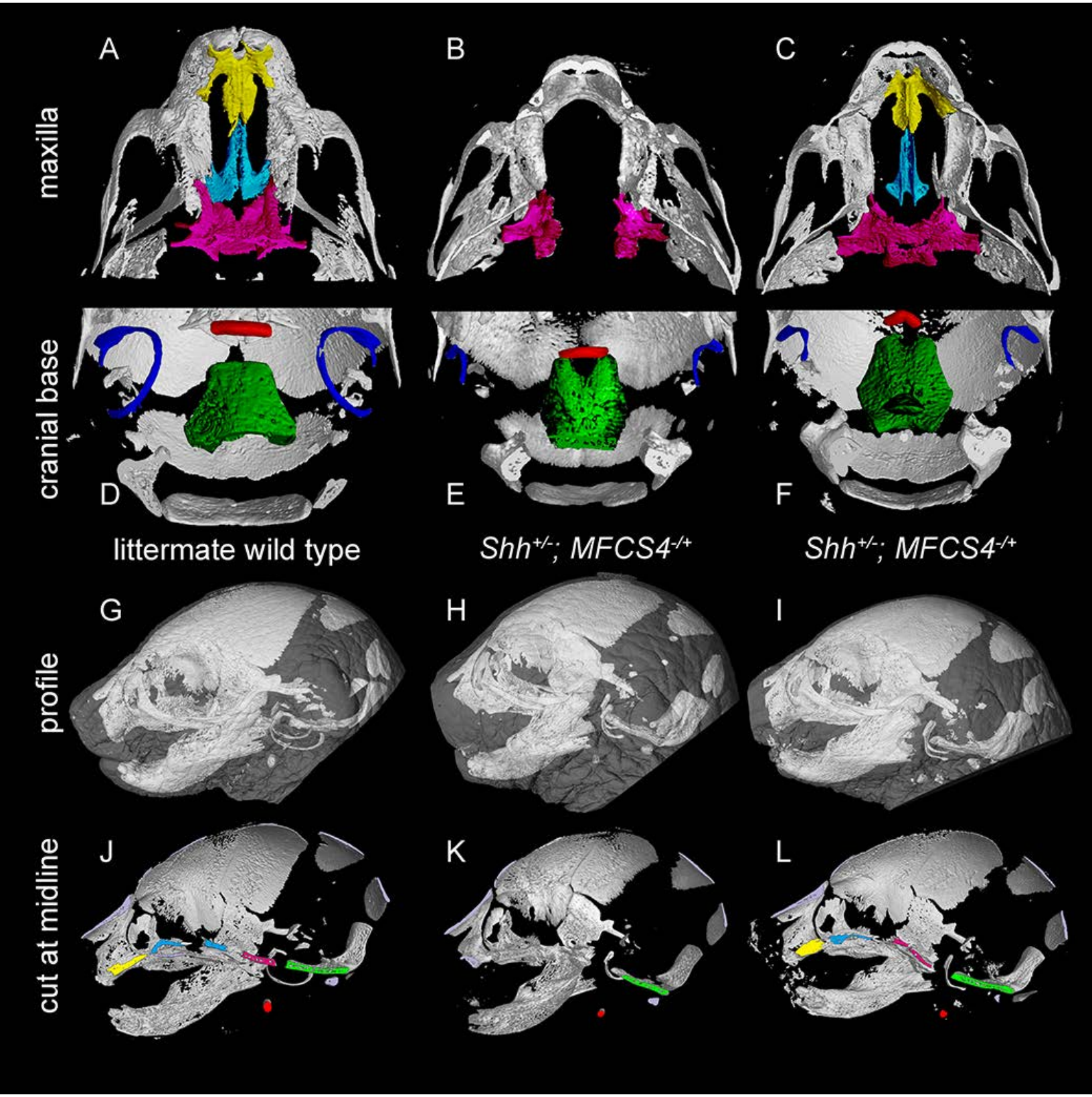
A
B
C
maxilla
cranial base
D
E
F
littermate wild type
Shh+/-; MFCS4-/+
Shh+/-; MFCS4-/+
G
H
I
profile
J
K
L
cut at midline